POINT MASS METHOD APPLIED TO THE REGIONAL GRAVIMETRIC DETERMINATION OF THE GEOID

C. ANTUNES[1], R. PAIL[2], J. CATALÃO[1]

1 Laboratory of Tectonophysics and Experimental Tectonics, Faculty of Sciences, University of Lisbon, Lisbon, Portugal (cmantunes@fc.ul.pt)
2 Department of Theoretical Geodesy, Institute of Geodesy, Graz University of Technology, Graz, Austria (pail@geomatics.tu-graz.ac.at)

Received: September 9, 2002; Accepted: February 13, 2003

ABSTRACT

The determination of the local gravity field by means of the point mass inversion method can be performed as an alternative to conventional numerical methods, such as the least-squares collocation. Based on the first derivative of the inverse-distance Newtonian potential for the representation of the gravity anomaly data, it is possible to compute any wavelength component of the geoid in planar approximation with sufficient accuracy. In order to exemplify the theoretical concept, two applications are presented of the computation of two different wavelength components of the geoid, the long wavelength component in a local solution and the short wavelength component in a regional solution. The results are compared with corresponding least-squares collocation solutions, using a global geopotential model to remove and to restore the long wavelength component.

Keywords: point mass method, least-squares collocation, planar approximation, gravity anomaly, trend field, Tagus Valley, Azores

1. INTRODUCTION

The geoid is one of the most important reference surfaces for geodesists. During the past decade the need for better geoid models has been driven by the increased use of the Global Position System (GPS) for point positioning. GPS users need to convert the ellipsoidal height to the local orthometric height through a geoid model; for height determination it is required that the accuracy of geoid models is comparable with that of the GPS. Therefore, refined geoid models have been computed all over the world with gradually increasing accuracy and precision.

Most of the geoid models were mainly determined by two different methods: numerical integration and least-squares collocation. These two methods are well established and documented, and there exists generally available software for their implementation, which makes them the best known and most widely used by the geodetic community.

The point mass inversion method may be viewed as an alternative method for gravity field modulation. *Weightman (1965)* was one of the first to suggest the use of point masses in physical geodesy. The idea to search for alternatives to the classical representation of the gravity field in terms of spherical harmonics lead many authors (*Needham, 1970; Balmino, 1972,1974; Reilly and Herbrechts, 1978; Sünkel, 1981,1983; Heikkinen, 1981; Freeden, 1983,1987; Forsberg, 1984; Hauck and Lelgemann, 1985, Barthelmes, 1986; Vermeer, 1989,1990; Vermeer and Forsberg, 1992; Lehmann, 1993, 1995; Vajda and Vaníček, 1997*) to investigate a variety of methods based on point masses. The methods differ from one another mainly in the strategy of determining the point mass position. While using fixed positions seems to be preferable due to their simplicity and fast computation, in some situations these methods may have some numerical instability.

Dampney (1969) shows that it is possible to fit a gravity data set by computation of the gravity effect of a set of point masses (equivalent sources) positioned exactly beneath the gravity data points. The proposed method involves a linear system and is solved for the point masses by inverting a matrix with the same dimension as the amount of data. It should be pointed out that point mass inversion in this case can be considered to be equivalent to least-squares collocation when the Poisson covariance function is used (*Moritz, 1980*).

Cordell (1992) presents a simple iterative algorithm for the determination of the point mass value. Instead of using the first derivative of the disturbing potential associated with gravity (used by *Dampney, 1969*), this author suggests the adjustment of the gravity anomaly data set with the inverse-distance Newtonian potential function. This solution of point masses results from an iterative procedure, and appears to be a simpler and faster as compared to the linear equation system presented by *Dampney (1969)*. Besides their differences in implementation, these two methods were specifically designed for interpolation of gravity anomalies.

Barthelmes (1986) designed an algorithm for optimizing point masses with free positions based on a least-squares adjustment with four free parameters per point mass. The method results in a small number of point masses, making the evaluation of the functional much faster, but it is computationally demanding due to the developed numerical strategy.

In the present paper, we present a strategy based on Cordell's algorithm applied to the functional used by Dampney (the first derivative of the inverse-distance Newtonian potential), for the local and regional gravimetric determination of the geoid. In the previous work (*Antunes et al., 2000*) we reported an alternative approach for the gravimetric determination of the geoid presented in this paper; this was done with a different functional representation but with similar results. First, this technique is applied to the local determination of the geoid to compute the trend field of the gravity to be used in the remove-restore technique (*Forsberg and Tscherning, 1981*) in an effort to obtain a homogeneous and isotropic signal field for the correct application of the **L**east-**S**quares **C**ollocation (*Moritz, 1980*). Second, it is applied to computing the signal of the geoid in substitution of the LSC, using exactly the same numerical steps in a similar way as in the LSC method. These two approaches are explained in Sections 3.1 and 3.2, respectively.

Our simple idea enables the computation of any spectral component of the geoid that results from the integration of the functional fitted to the respective component of the

gravity data. In principle this method can be applied in any coordinate frame, but for the sake of simplicity we have limited this study to a planar approximation.

2. POINT MASS METHOD FOR THE DETERMINATION OF THE GEOID

We will use two steps to define the concept of the determination of any geoid wavelength component by the point mass method. First, we show how the gravity anomaly data can be synthetically generated by a functional that depends on the initial gravity data, on the position and on the magnitudes of the point masses. Second, we show the transformation of this functional to the functional that will synthetically represent the respective geoid wavelength component from the same source set.

The gravity anomaly generated by a set of M perturbing point masses in planar approximation may be expressed as (*Dampney, 1969*):

$$\Delta g(x_i, y_i, z_i) = G \sum_{k=1}^{M} \frac{c_k (z_i - \zeta_k)}{\left((x_i - \xi_k)^2 + (y_i - \eta_k)^2 + (z_i - \zeta_k)^2\right)^{3/2}}, \tag{2.1}$$

where G is the gravitational constant, c_k ($k = 1, \ldots, M$) are the point-mass magnitudes and $\{\xi_k, \eta_k, \zeta_k\}$ are the point-mass coordinates. This function can be fitted to a gravity anomaly data set of discrete measurements with coordinates $\{x_i, y_i, z_i\}$, for i running from 1 to N data points, and a set of point masses can be determined accordingly with specific a priori conditions. The planar coordinate system is defined as a local right-handed Cartesian system with the z axis pointing upwards and with its origin at geoid level ($z = 0$, sea level).

Due to the non-uniqueness of the inverse problem of the potential theory, in principle there are infinitely many different sets of sources representing the same gravity field, which means that with a set of gravity anomalies it is impossible to find uniquely the anomalous mass distribution. Throughout, the anomalous mass distribution must be determined in a trial and error forward model imposing a priori conditions (point-mass depth or point-mass planimetric position) and solved iteratively until an apriori error limit is obtained. There are several algorithms used to solve this problem, and we have adopted Cordell's strategy (*Cordell, 1992*), with a different gravity anomaly function.

Following Cordell's algorithm, the set of point masses is constructed iteratively, adding one source at a time. At each iteration step, k, the constant value c_k is computed from the largest absolute value of the gravity anomaly data

$$\left|\Delta g_{i_m,k}\right| = \max\{\left|\Delta g_{i,k-1}\right|\} \tag{2.2}$$

after removing the effect of the sources of the earlier iterations, and such that:

$$\Delta g_{i_m,k} = G\, c_k \zeta_k^{-2} \tag{2.3}$$

This simple formula (2.3) yields the set of point-mass magnitudes $\{c_k\}$ that results from equation (2.1) considering each source to be placed beneath the maximum $\left|\Delta g_{i_{\max}}\right|$, and assuming the gravity anomalies to be given at sea level ($z_i = 0$). In this formula the value of parameter ζ_k, corresponding to the depth of the source, still has to be defined. For

the sake of simplicity, we define it here as a fixed depth for all sources, i.e. ζ_k represents a constant; a strategy that turns out to be sufficient for our applications. In *Cordell (1992)* the source depth is defined as a variable proportional to the distance to the nearest neighbouring data point.

At each iteration step, the effect of the respective source is removed from all data, as follows:

$$\{\Delta g_{i,k}\} = \left\{ \Delta g_{i,k-1} - \frac{G\, c_k (\xi_i - \xi_k)}{\left[(x_i - \xi_k)^2 + (y_i - \eta_k)^2 + (z_i - \zeta_k)^2\right]^{3/2}} \right\}_{i=1,N} \tag{2.4}$$

yielding a residual field. In the next iteration step, $k + 1$, the maximum $\Delta g_{i_{\max},k+1}$ is again sought over the residual field. Then we fit a new source by (2.3) and again remove the respective effect until the process stops at a previously defined maximum number of iterations Q, or alternatively if the cut-off criterion of $\max |\Delta g_{i,k}| < \varepsilon$ is fulfilled, where ε is a previously defined small number.

The iterative process is usually convergent, depending on the chosen depth for the sources and the distribution of the data. This approach yields a set of point masses, where the potential effect approximates the gravity anomaly data (2.1) with the desired accuracy given by the expression

$$\sigma = \sqrt{\frac{\sum_{i=1}^{N} (\Delta g_{i,M})^2}{N}}\,, \tag{2.5}$$

where $\Delta g_{i,M}$ is the residual field after M iterations, removing successively the effect of each source from the data, and N is the number of data points.

Therefore, after Q iterations we arrive at Q point masses, and because every data point is repeatedly considered in all iterations, more than one mass may occur beneath a given data point. In this case, these point masses beneath the same point can be combined by superposition, and we end up with a number M of masses, which is smaller than the number of data points N.

This is the algorithm to compute the set of point masses that generate the synthetic gravity anomalies through formula (2.1).

From the spherical approximation of the fundamental equation of physical geodesy (*Heiskanen and Moritz, 1967, p. 88*), assuming $\partial/\partial r = \partial/\partial z$, the formula for the planar approximation of this boundary condition can be obtained as

$$\Delta g(x,y,z) = -\frac{\partial T(x,y,z)}{\partial z} + \frac{\partial \gamma(x,y,z)}{\partial z} N(x,y,z) \tag{2.6a}$$

For some order of approximation we can disregard the second term on the right-hand side of the fundamental equation of geodesy (2.6a), and approximate the gravity anomaly by gravity disturbance. Under this assumption (2.6a) can be modified to read

$$\Delta g(x,y,z) \cong -\frac{\partial T(x,y,z)}{\partial z} \tag{2.6b}$$

For both of our applications it can be proved that neglecting such a term has no significant effect on the results. In the first application, shift-fitting the solution to benchmarks with known geoid undulations remove the effect. However, for larger areas or for areas with large topographic irregularities this term must be considered, for example by converting the gravity anomalies into gravity disturbance using an estimated value for the vertical gradient of the normal gravity and the geoid undulation from the first computation. For the signal determination case, once the remove-restore technique with EGM96 is applied, the effect of neglecting such a term in the determination of the residual component is negligible. The estimate of the omitted term is less than 0.6 mGal, approximately of the same magnitude as the accuracy given by (2.5) of the point-mass method fitting.

Assuming (2.6b) to be valid, the anomalous gravity potential T, by integrating with respect to z, will be defined by the inverse-distance Newtonian potential as:

$$T(x,y,z) = G\sum_{k=1}^{M} \frac{c_k}{\sqrt{(x_i-\xi_k)^2+(y_i-\eta_k)^2+(z_i-\zeta_k)^2}} \tag{2.7}$$

Even though this formula is valid for outer space, for the determination of the geoid we just need to compute it at the geoid level ($z = 0$). Finally, using Bruns' formula (*Heiskanen and Moritz, 1967, p.85*), yields the functional for determining the geoid undulation:

$$N(x,y) = \frac{G}{\gamma}\sum_{k=1}^{M} \frac{c_k}{\sqrt{(x-\xi_k)^2+(y-\eta_k)^2+\zeta^2}} \tag{2.8}$$

Assuming that the set of sources $\{c_k(\xi_k, \eta_k, \zeta)\}$ does not represent the whole gravity anomaly field, but just a certain spectral component of it, this functional (2.8) will only yield the respective spectral component of the geoid undulation. This statement justifies our applications in Sections 3.1 and 3.2, where we apply this technique to a certain spectral component only.

Resuming the procedure: first determine the set $\{c_k\}$ of sources using (2.3) with condition (2.2) by an iterative process, where the potential effects of the point sources are removed from the gravity anomaly values by (2.4). The iterative process will stop either after a previously defined maximum number of iterations, or when a certain accuracy of approximation is reached. Convergence is achieved by experimenting the optimum depth values (ζ) for the sources, according to the convergence of the precision value (σ) given by (2.5) and to the irregularities of the field. We have observed that the rate of convergence of the method using the first derivative, as we do here, instead of the zero derivative of the inverse-distance Newtonian potential for the representation of gravity anomalies (*Antunes et al., 2000*), is lower, and the convergence is more sensitive to the chosen depth of the sources, making it more unstable.

After the determination of the point-mass set, we only have to compute the respective geoid wavelength component using (2.8).

3. TEST CASES AND DATA

In order to verify the applicability of this method, we have used two different test areas. As an application of the method to trend determination we have used a sample of 640 gravimetric points of the Portuguese gravimetric network of Instituto Português de Cartografia e Cadastro (IPCC) in the region of Lisbon and the Tagus Valley (Fig. 1). This is located between latitudes $\varphi = 38.4°$ and $\varphi = 39.4°$, and longitudes of $\lambda = -9.5°$ and $\lambda = -7.9°$, and the average station density there is 1 point/4 km^2.

Due to the absence of a precise local digital terrain model, the topographic global model ETOPO5U was used to compute the topographic and isostatic corrections. Additionally, to evaluate the final precision and to adjust the geoid model, 8 geoid undulations observed by GPS and precise levelling were used. The global geopotential model used to compare the results was EGM96 (*Lemoine et al., 1997*).

For the determination of the geoid signal we used a set of a 6570 data points in the central group of the Azores archipelago (Fig. 2), from a database of the Azores region (*Catalão and Sevilla, 1999*). This database was composed of the following sources: a) ERS altimetric data from 32 days and 168 day cycles; b) EGM96 geopotential model; c) AZDTM98 digital terrain model, and d) gravity anomalies previously validated and obtained from shipboard measurements.

The original database, which was composed and used in previous studies (*Catalão and Sevilla, 1998*), resulted from a compilation of BGI, NGDC and DMA databases. Most of the data were acquired from US, UK and French institutions in the period from 1970 to 1990. The gravity data was validated by crossover error adjustment fixing the longest track from United Kingdom. This database was improved with one more gravimetric campaign performed in 1997 in the framework of the PDIC/C/Mar project (*Fernandes et al., unpublished data*). A new crossover adjustment was made considering the PDIC/C/Mar tracks to be error free. After adjustment, the standard deviation of the crossover error dropped to 2.61 mGal (from an initial value of 7.21 mGal). In order to cover the remaining areas with poor data coverage, satellite derived gravity anomalies from *Andersen and Knudsen (1998)* were combined with observed gravity anomalies.

To fit the solution and to verify the final precision, the MSS95 was used on the sea, and geoid undulations observed by GPS and levelling in São Miguel Island.

These two data sets will be used in the two practical applications described in the next sections, the trend and the signal determination.

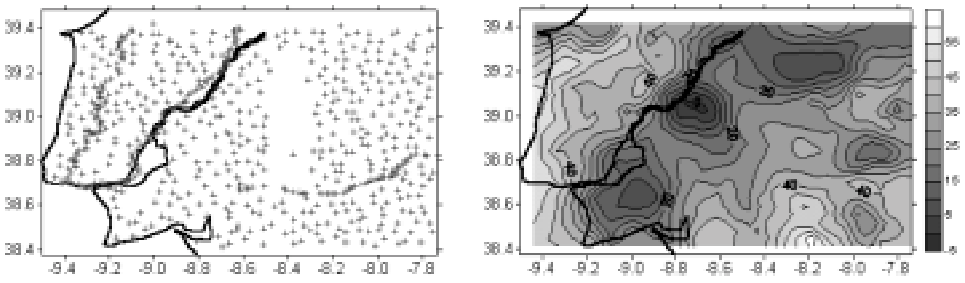

Fig. 1. Point distribution and topo-isostatic reduced gravity anomaly map (Tagus Valley).

3.1. Trend determination

The LSC in determining the regional or local geoid must be applied in combination with the remove-restore technique to remove the trend component (the long wavelength or systematic component) from the input data, transforming it into a homogeneous signal. Additionally, we must take into consideration the type of covariance model to be used, either a global model, locally adjusted, or a plane covariance function. The plane covariance functions are usually homogeneous and isotropic, i. e. invariant to translations and rotations, respectively. Our concern in this specific application was to prove the influence of the homogeneity and isotropy of the empirical covariance in the LSC solution when it is applied to such small areas as the Tagus Valley.

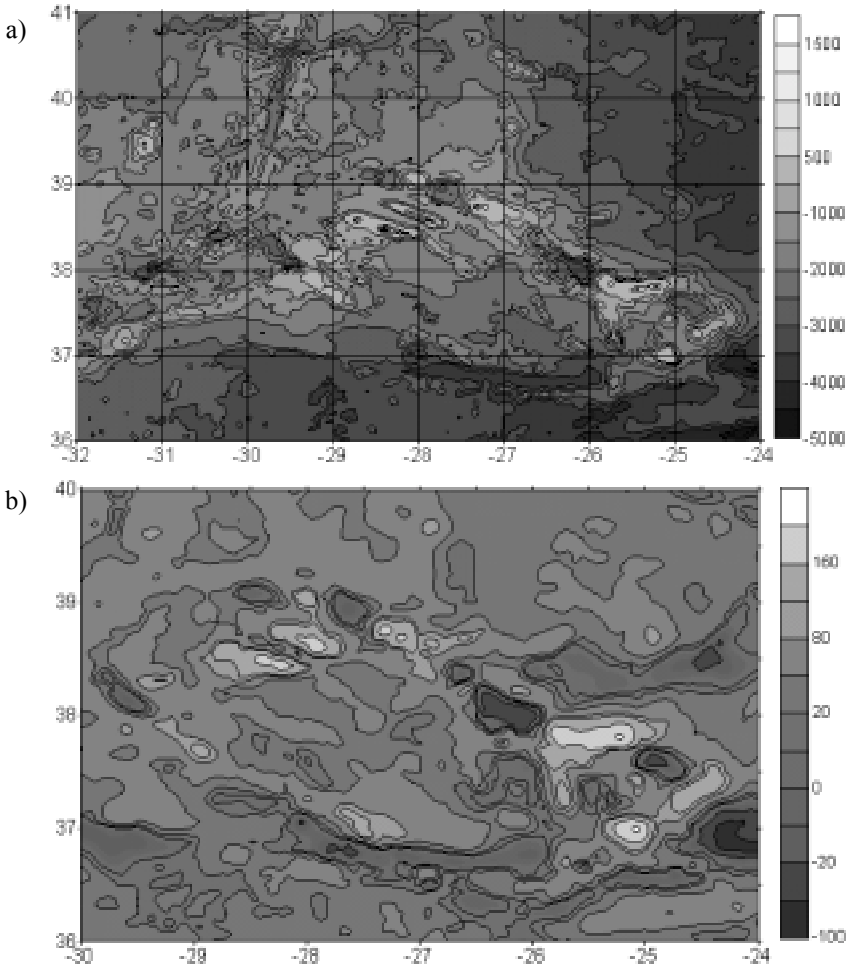

Fig. 2. a) AZDTM98 bathymetric/altimetric map contoured every 500 m (Azores); b) Free air gravity anomalies map (contour interval is 20 mGal).

In this study we have compared the results from two configurations: one using a global geopotential model and the other, using a local trend model determined by the point-mass method to remove the long wavelength component of the data.

It is known that for small areas, with the same dimension as the resolution of global models ($1° \times 1°$), after removing a global geopotential model, the residual field is neither homogeneous, nor isotropic. In this situation a planar covariance function does not yield good results, because it cannot be fitted exactly to the empirical covariance, and consequently, it introduces errors in the solution. Therefore, we have tried a combined technique that enables the determination of a local trend model of gravity anomalies, and after removing it from the original data the residual field will be centred, homogenous and isotropic (*Antunes, et. al., 2000a*). Since the trend, represented by a functional such as (2.1), is differentiable, we can recover the respective trend of the geoid undulations from (2.8).

This combined technique is the result of combining a low-pass filter with the point-mass method. The purpose of the previous application of a low-pass filter is to remove the short wavelength effect, leaving only the trend component to be fitted by the point-mass algorithm. A simple linear low-pass filter is sufficient to remove the high frequencies, and for this reason we have designed a filter with the following spectral characteristics:

$$\begin{aligned} H(\omega) &= 1, && \omega \le \omega_{c1} \\ H(\omega) &= 1 - \frac{\omega - \omega_{c2}}{\omega_{c1} - \omega_{c2}}, && \omega_{c1} > \omega > \omega_{c2} \\ H(\omega) &= 0, && \omega \ge \omega_{c2} \end{aligned} \tag{3.1}$$

In the present application, the filter cut-off frequency $(\omega_{c1} + \omega_{c2})/2$ corresponds to a wavelength of 58 km, which is half of the smallest dimension of the area. In analogy to formulas (2.1) and (2.8), the trends for the gravity anomaly and geoid undulation of the same potential field corresponding to the filtered field are represented by:

$$t_{\Delta g_i}(x_i, y_i) = -G \sum_{k=1}^{M} \frac{c_k \zeta}{\left((x_i - \xi_k)^2 + (y_i - \eta_k)^2 + \zeta^2\right)^{3/2}}, \tag{3.2}$$

$$t_{N_i}(x_i, y_i) = \frac{G}{\gamma} \sum_{k=1}^{M} \frac{c_k}{\sqrt{(x_i - \xi_k)^2 + (y_i - \eta_k)^2 + \zeta^2}}, \tag{3.3}$$

where the M magnitudes c_k are iteratively computed by Cordell's algorithm from the filtered data.

The application of the filter (3.1) to the data presented in Fig. 1 results in a discrete trend field on a grid, to which we apply the point-mass algorithm, resulting in a similar but synthetic field, now represented by the harmonic functional (3.2). This functional, with such a set of point masses determined by the point-mass method represents the trend component of the input gravity anomaly field, where only wavelengths greater than 58 km are present. Applying the remove-restore technique by using this local trend model, we split the original gravity anomalies into two components, the trend and the signal (Fig. 3).

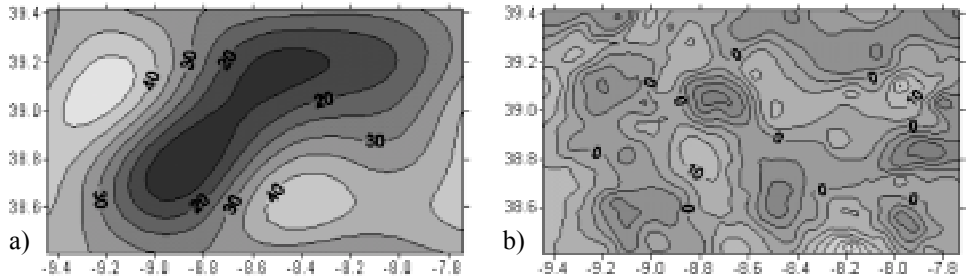

Fig. 3. Decomposition of the input gravity anomalies. a) Local trend model for gravity anomalies; b) residual field (in mGal), in the Tagus Valley.

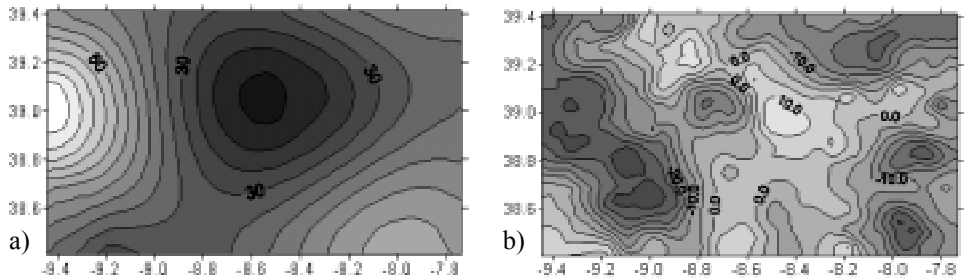

Fig. 4. Decomposition of the input gravity anomalies. a) EGM96 model for gravity anomalies; b) residual field (in mGal), in the Tagus Valley.

The edge effects of the spectral filtering, due to the lack of surrounding data, is a problem we have to face in this application. In order to minimise this effect we can fill the surrounding area with data, such as predicted data, and use only the inner part to compute the local trend field. A second problem is the lack of regional information, leading to a local trend solution determined by local data, which does not represent the regional behaviour correctly. It implies a fitting of the final solution by direct geoid undulation observations in the inner and surrounding zones.

Fig. 4 shows the same decomposition applied to the global potential model EGM96 for the same test area. Comparing Figures 3 and 4, the differences can easily be seen. Concerning the trend component, there are differences corresponding to the shape of the main feature along the Tagus River. The edge effects result from the application of the filter due to the lack of surrounding data. Considering the high-frequency signal, there are differences in homogeneity that can be proved by the empirical covariance of both signals. Studies on the power spectrum of both signals also indicate a lower anisotropy of the residual field resulting from the application of the local trend (*Antunes et al., 2000*). The reason is obvious, because the global model EGM96 does not remove the trend from the data in such a small area completely. This was the main goal that led us to study these local solutions.

Let us now verify the differences in the solution of the LSC (Fig. 5) applied to both signals, with the same covariance model (3.4). The covariance function used in this application (*Hirvonen, 1962*), known as the Hirvonen function, is an example of the

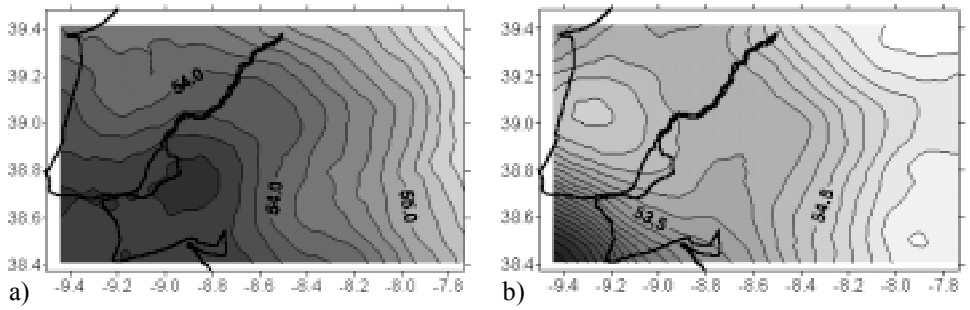

Fig. 5. Geoid solutions with the plane covariance model. a) using local trend model; b) using the EGM96 global model.

homogeneous and isotropic covariance function, invariant to translations and rotations (*Moritz, 1980, p.180*),

$$K(P,Q)=\frac{C_0 b^2 (z+z'+b)}{\left[\rho^2+(z+z'+b)^2\right]^{3/2}} \tag{3.4}$$

The analysis of the error covariance matrix indicates a variance of the local trend solution of 0.14 m^2, in contrast to 0.20 m^2 for the EGM96 solution. It shows that guaranteeing the homogeneity and isotropy of the empirical covariance is important in the prediction by LSC, if such a planar covariance function is used. These variances do not yet reflect the final accuracy of the geoid models, because the accuracy of the local trend model has not been yet verified. The 8 geoid heights observed in this area make this test and the respective local adjustment possible.

We may observe two important facts in the improved solution: lower amplitude related to the lack of the regional information, and an incorrect mean value (not present in the figure) related to the ambiguity of the integration constant in (2.8). This constant was simply determined using a directly observed undulation.

For comparison we have computed a third solution using the EGM96 (Fig. 6) and a locally adjusted global covariance, assuming it to be the best geoid solution for our data, because such a covariance model solves the problem of the homogeneity and isotropy correctly. Table 1 compares the results and provides the respective statistics of the three solutions: 1) using the local trend model determined by the point-mass method and a planar covariance model; 2) using EGM96 and the planar covariance model; and 3) using EGM96 and a global covariance model adjusted locally. Comparing the first two solutions, the local trend model solution is much more accurate, and comes very close to the best solution that uses a locally adjusted global covariance function.

Table 1 clearly shows that planar covariance functions cannot be applied to the residual field resulting from the de-trending of geopotential global models, due to the inhomogeneity and the anisotropy of its empirical covariance function. Whereas the solution resulting from the local trend model determined by the point-mass method is very close to the solution resulting from global models. This provides a very important

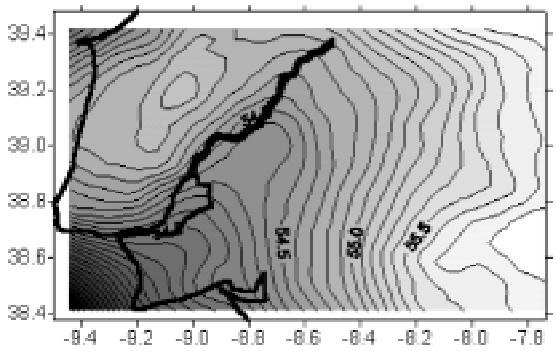

Fig. 6. The Tagus Valley geoid solution using EGM96 and a global covariance model adjusted locally.

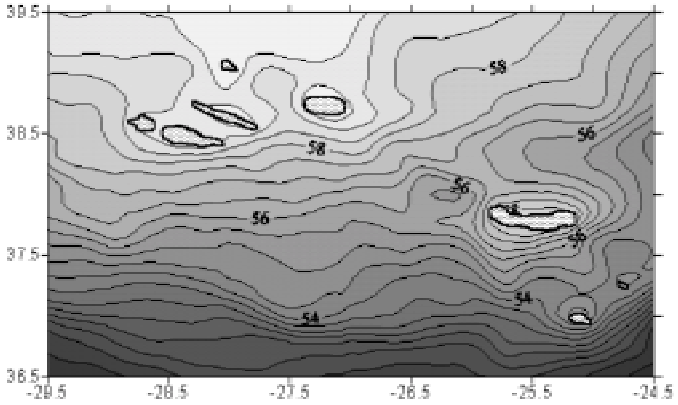

Fig. 7. Gravimetric geoid model (in metres) around the Azores archipelago determined by the point-mass method.

conclusion: with simple mathematical formulation it is possible to compute local geoid solutions using local data only.

3.2. Signal determination

Our effort to apply this technique for geoid determination in substitution of the LSC method, was prompted by the simplicity of this method, its low running time and the low memory capacity required for the computation.

The methodology followed here is the same as that used in the LSC for determining the geoid (*Tscherning, 1985*). After removing the long wavelength component of the gravity field and the very short wavelength component of the topography, we apply the point-mass method to the residual field.

Does the method numerically maintain the gravity field structure maintained by the LSC? Of course it does, the analytical structure is preserved since the set of masses

Table 1. Comparative analyses of the solutions (in metres), before and after an adjustment by 8 direct undulation observations from the Tagus Valley area.

Solutions	Before Adjustment				After Adjustment			
Trend + Covariance	Min	Mean	Max	Std	Min	Mean	Max	Std
LOCAL + Planar	0.11	0.22	0.83	0.23	–0.14	0.00	0.18	0.11
EGM96 + Planar	–0.47	–0.13	0.69	0.37	–0.40	0.00	0.33	0.26
EGM96 + Global	–0.92	–0.77	–0.59	0.10	–0.15	0.00	0.08	0.07

$\{c_k(\xi_k, \eta_k, \zeta)\}$ is the same in the whole process, and the kernel functional used has the same properties (harmonic, regular, homogeneous and isotropic) as the one used in the LSC. Therefore, once the analytical structure is preserved, the method can indeed be an alternative to the LSC if it yields a solution with a precision comparable to the LSC solution. In order to prove these aspects we performed a comparative study with the LSC solution, using the gravity data of the Azores region.

Comparing this application for the medium wavelength component to the earlier application for the local trend model, this is a much simpler problem in the sense that we do not have to perform any specific pre-processing, such as filtering, to apply the point-mass method. This means that we only have to fit the residual gravity anomalies to the first derivative of the inverse-distance Newtonian potential function using the Cordell iterative process, and then compute the respective geoid wavelength component using functional (2.8) and the same set of masses $\{c_k(\xi_k, \eta_k, \zeta)\}$.

The fitting of the gravity anomalies by an iterative process and the final geoid computation applying (2.8) are the only two steps, which demonstrates the simplicity of computation for the signal component of the geoid by the point-mass method. Concerning the computational effort, let us just consider the large number of operations for matrix computation that has to be performed in the LSC, and the corresponding increase of the matrix dimension with the enlargement of the area for geoid computation. As we know, the matrix dimension in the LSC applied to a large amount of data is one major inconvenience of this method. It proves clearly that the method presented here is much simpler and considerably faster.

Table 2 shows the statistics of the two solutions and their differences, and Table 3 shows the statistics by comparing the solutions with the GPS heights on land and with the Sea Surface Height (SSH) on the sea. With these numerical results we show that the point-mass method, as it is tested here, yields numerical solutions nearly identical as the collocation method.

4. DISCUSSION AND CONCLUSIONS

The point-mass method was applied and evaluated in two different study cases: first, in the trend determination in the local gravity field (in Lower Tagus valley) as a

Table 2. Statistics of both the geoid solutions (in metres) and their difference for the Azores area.

Solutions	Min	Mean	Max	Std
Collocation	49.80	55.93	60.20	2.62
Point Mass	48.64	54.78	59.11	2.63
Collocation – Point Mass	1.02	1.15	1.29	0.05

Table 3. Statistics of the differences (in metres) between geoid models and SSH from ERS-1, on sea, and GPS heights on land.

Differences	Original				Fit
	Min	Mean	Max	Std	Std
GeoidCol – SSH(MSS95)	–0.47	–0.09	0.64	0.16	0.13
GeoidPM – SSH(MSS95)	0.35	0.74	1.40	0.16	0.12
GeoidCol – GPS(S.Miguel)	–1.38	–1.01	–0.30	0.29	0.07
GeoidPM – GPS(S.Miguel)	–1.31	–0.96	–0.23	0.29	0.11

substitution of the global geopotential models, and second, in the regional geoid determination in the Azores region.

In both applications topographic corrections were applied to the free-air anomalies, in order to satisfy the conditions of the boundary value problem applied to the regularised geoid. The indirect effects were taken into account by restoring the respective corrections. The same remove-restore technique was used for de-trending the gravity field model, and it was applied either with the global geopotential model (EGM96) or with the local trend model computed by the methodology described in Section 3.1.

Due to the lack of knowledge of the mean value of the geoid in both the test areas, and particularly to solve the unknown integration constant in Section 3.1, it was necessary to make an adjustment to each solution by means of control points. Additionally, the fact that a planar approximation is used and the geoid is solved for a local or regional area imposes a certain kind of adjustment. This adjustment can also be used to verify the precision and accuracy of the models. On land direct undulation observations obtained by GPS and levelling were used, and on the sea the Mean Sea Surface of 1995 (MSS95) was applied.

Applying this method for determining the trend of the local solutions was justified by the fact that the empirical covariance of the residual field, obtained by removing the trend using global geopotential models in small areas such as $1° \times 1°$, is neither homogeneous, nor isotropic. In such a case we cannot use homogeneous and isotropic analytical models of the covariance function in the LSC in the proper way. In order to apply this method for trend determination, a low-pass filter was applied to remove the short wavelength from the data, retaining only what can be considered as the trend for such an area. Following this step, the point-mass method was applied to the long wavelength component of gravity

anomaly in order to determine the trend in terms of harmonic representation to be used in the remove-restore technique in the LSC application. This task was performed in the lower Tagus Valley region, near Lisbon, Portugal.

In the first application, the trend field model determination by the point-mass method shows some disadvantages, i.e., the regional behaviour of the field and the determination of the integration constant. But in order to obtain a homogeneous and isotropic empirical covariance, these disadvantages are easily overcome by direct undulation observations, which must be well distributed over the test area. We have proved the idea that the homogeneity and isotropy of the empirical covariance function must be considered, and only with local data does this strategy turn out to be possible for determining a high-quality geoid model.

We can also conclude that by applying this method we have only achieved a higher accuracy of the short wavelength component, the signal, but simultaneously reduced the accuracy of the long wavelength component, the trend. However, in the absence of good global models for the geopotential and for the covariance function we end up with an acceptable method.

The prediction of the geoid signal by the point-mass method resulted in an alternative method to the LSC in regional gravimetric geoid determination, which is much simpler and faster. Comparing the results obtained for the tested area, the Atlantic region of the Azores, with the LSC solution, they turn out to be quite similar both in precision and in accuracy.

In the second application, if we compare both the solutions after fitting them to the SSH (Table 2), we can conclude that they provide results which are similar both in precision and accuracy. Considering the computation time (few minutes versus few hours or more), the memory requirements (iterative process versus a large matrix computation), the simplicity and the results of both methods, we conclude that the point-mass method appears to be a good method for local and regional gravimetric geoid determination.

The disadvantages of the proposed method, when compared to the collocation method, are related to the absence of a stochastic model and the impossibility of data combination (gravity anomalies, deflections of the vertical and geoid undulations). While the first disadvantage can be overcome by predicting the precision by adjustment with direct undulation observations, the second disadvantage cannot be overcome because it is a feature only of statistical methods such as the least-squares collocation, which makes it really suitable and preferable to other methods.

These conclusions lead us to propose the point-mass method as a fast alternative method to collocation for local and regional gravimetric geoid determination, and under certain conditions also a good method for local trend model determination in combination with low-pass filtering.

Acknowledgements: We sincerely thank the IPCC for providing us with the gravity anomaly data, and we are especially indebted to J. Teixeira Pinto and Helena Koll for their invaluable help.

References

Andersen O.B. and Knudsen P., 1998. Global marine gravity field from ERS-1 and Geosat geodetic mission altimetry. *J. Geophys. Res.*, **103**, 8129–8137.

Antunes C., Pail R. and Catalão J., 2000. Determinação de um campo tendência Local, comparação com o modelo global EGM96. *Actas da II Conferência Nacional de Cartografia e Geodesia*, 23 e 24 de Setembro de 1999. IPCC, Lisboa, Junho de 2000, 311–319.

Barthelmes F., 1986. *Untersuchungen zur Approximation des äußeren Gravitationsfeldes der Erde durch Punktmassen mit optimierten Positionen*. Veröff. D. Zentr. Inst. F. Phys.d. Erde, Nr. **92**, Postdam.

Catalão J. and Sevilla M.J., 1998. Geoid studies in the north-east Atlantic (Azores-Portugal). In: R. Forsberg, M. Feissel and R. Dietrich (Eds.), *Geodesy on the Move*. Proceedings of the IAG Scientific Assembly, Rio de Janeiro, Sept. 3–9, 1997, Springer-Verlag, 269–274.

Catalão J. and Sevilla M.J., 1999. The effect of high precision bathymetric model on geoid computation. *IGS Bulletin*, **10**, 91–99.

Cordell L., 1992. A scattered equivalent-source method for interpolation and gridding of potential-field data in three dimension. *Geophysics*, **57**, 629–636.

Dampney C., 1969. The equivalent source technique. *Geophysics*, **34**, 39–53.

Forsberg R. and Tscherning C.C., 1981. The use of height data in gravity field approximation by collocation. *J. Geophys. Res.*, **86**, 7843–7854.

Heiskanen W.A. and Moritz H., 1967. *Physical Geodesy*. W.H. Freeman and Company, San Francisco, USA.

Hirvonen R.A., 1962. *On Statistical Analysis of Gravity Anomalies*. Publ. Isostat. Inst. Int. Assoc. Geod., No. **37**, Helsinki, Finland.

Lehmann R., 1995. Gravity field approximation using point masses in free depths. *Bulletin 1 of IAG*, 129-140.

Lemoine F.G., Smith D.E., Kunz L., Smith R., Pavlis E.C., Pavlis N.K., Klosko S.M., Chinn D.S., Torrence M.H., Williamson R.G., Cox C.M., Rachlin K.E., Wang Y.M., Kenyon S.C., Salman R., Trimmer R., Rapp R.H. and Nerem R.S., 1997. The development of the NASA GSFC and NIMA Joint Geopotential Model. In: J. Segawa, H. Fujimoto and S. Okubo (Eds.), *Proceedings of the International Symposium on Gravity, Geoid and Marine Geodesy, GRAGEOMAR*, The University of Tokyo, Tokyo, Sept. 30 – Oct. 5, Springer-Verlag, 461–469.Moritz H., 1980. *Advanced Physical Geodesy*. H. Wichmann Verlag, Karlsruhe, Germany.

Tscherning C.C., 1985. Local approximation of the gravity potential by least squares collocation. In: K.P. Schwarz (Ed.), *Proceedings of the International Summer School on Local Gravity Field Approximation*, Beijing, China, Aug. 21 – Sept. 4, 1984. Pub. 60003, Univ. of Calgary, Calgary, Canada, 277–362.

Vajda P. and Vaníček P., 1997. On the gravity inversion for point mass anomalies by means of the truncated geoid. *Stud. Geophys. Geod.*, **41**, 329–344.

Weightman J.A., 1965. Gravity, Geodesy and Artificial Satellites. A Unified Analytical Approach. *Proc. Symp. on The Use of Artificial Satellites for Geodesy*. Athen 1965.